

Capillary Microfluidic-Assisted Surface Structuring

Wei Li, Wenbo Sheng, Erik Wegener, Yunhao Du, Bin Li,* Tao Zhang,* and Rainer Jordan*

Cite This: *ACS Macro Lett.* 2020, 9, 328–333

Read Online

ACCESS |



Metrics & More



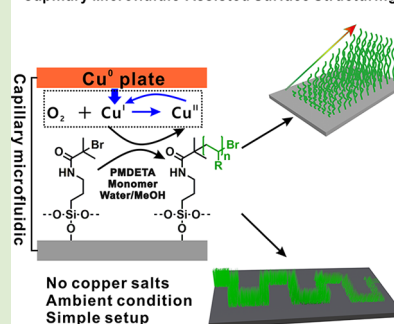
Article Recommendations



Supporting Information

ABSTRACT: A facile and universal oxygen-tolerant, capillary microfluidic-derived, controlled radical polymerization for surface structuring (gradient and patterned polymer brushes) is reported. A syringe pump and a filter paper sheet are used as capillary microfluidic to supply the reaction solution (monomer, solvent, and ligand) to a sandwich-shaped setup by placing a flat copper plate onto an ATRP initiator-modified substrate and resulting in gradient polymer brush formation with controlled thickness, steepness, and grafting area, polymers are showing the high chain-end fidelity. Two different polymer brushes (binary polymer brushes) can be simultaneously grown from both ends of the initiator modified substrate by using this method, which can be used to study the interfacial properties of different polymer brushes.

Capillary Microfluidic-Assisted Surface Structuring



Surface-initiated polymerizations (SIPs) provide a powerful approach to fabricate novel functional polymer brush coatings.^{1–3} However, conventional SIP technologies suffer from poor monomer efficiency, that is, several grams per mL of monomer only yield a nanometer-thick polymer brush layer, and the monomer is hard to purify and reuse, in particular, for the ionic monomers, which limit the scope of monomers and hinder their potential applications. To reduce the amount of monomer, microfluidic techniques have been exploited to prepare polymer brushes via the conventional atom transfer radical polymerization (ATRP) method, where a Cu^I/ligand complex is employed as the catalyst in an inert environment.⁴ For example, Tomlinson and Genzer prepared polymer brushes by draining a chamber with the ATRP reaction solution.⁵ Beers et al. developed a microchannel-confined surface-initiated ATRP method to synthesize gradient polymer brushes under the inert gas protection, gradient statistical copolymers were prepared via microfluidic techniques by mixing two monomers and following chamber filling.^{6,7} These methods reduced the usage of monomer solution while large amounts of copper salts are still needed as the catalyst, which limits its biologic applications due to the toxicity. Moreover, the use of oxygen-free reaction solutions requires tedious procedures (freeze–pump–thaw cycle or deoxygenation with inert gas), which severely limits the application of microfluidic-assisted polymer brush synthesis.

Among various polymer brush synthesis techniques,^{8–14} Cu(0)-mediated controlled radical polymerization (CuCRP) has attracted great attention because of its fast polymerization rate, highly living nature, and oxygen tolerance.^{15–19} By taking the advantages of CuCRP and ATRP method,^{20–23} we report a capillary microfluidic surface-initiated CuCRP (capillary μ SI-CuCRP) for the fabrication of structured polymer brushes on the planar substrate. To realize the capillary μ SI-CuCRP, a

syringe pump and a small piece of filter paper are used as capillary microfluidic to feed the polymerization solution to a sandwiched setup of the copper plate and the ATRP initiator-modified substrate. By continuously pumping the polymerization solution into the sandwiched system via the syringe, a [Cu^I]/[Cu^{II}] concentration gradient along the flow direction was formed and provided an effective mean in terms of controlling the polymerization kinetics during CuCRP.^{20–23} Therefore, gradient polymer brushes with controllable steepness, grafting area, and high end-group fidelity were prepared by adjusting the flow rate and the reaction time. Binary polymer brushes composed of two different polymers can be grown simultaneously from both ends of the substrate to the crossover when a filter paper was used, which can be used to study the interfacial properties of different polymer brushes and directed motility of droplets. By the virtue of paper cutting, complex polymer brush patterns (curve, array, triangle, Y shape, and complex logo) can be easily achieved.

Figure 1A shows the scheme of the pump-based capillary μ SI-CuCRP setup. A copper plate and an ATRP initiator-modified substrate were placed by facing each other and a commercial tape with a thickness around 260 μ m was used to generate a small gap between the two plates. The polymerization solution contains the monomer and ligand was injected into the inlet by a syringe. Afterward, the reaction solution wicked into the sandwiched system, the polymerization was carried out in the ambient atmosphere without degassing. Cu⁰ acts as a supplemental activator for the initiator R–X and as a

Received: November 21, 2019

Accepted: February 7, 2020

Published: February 18, 2020



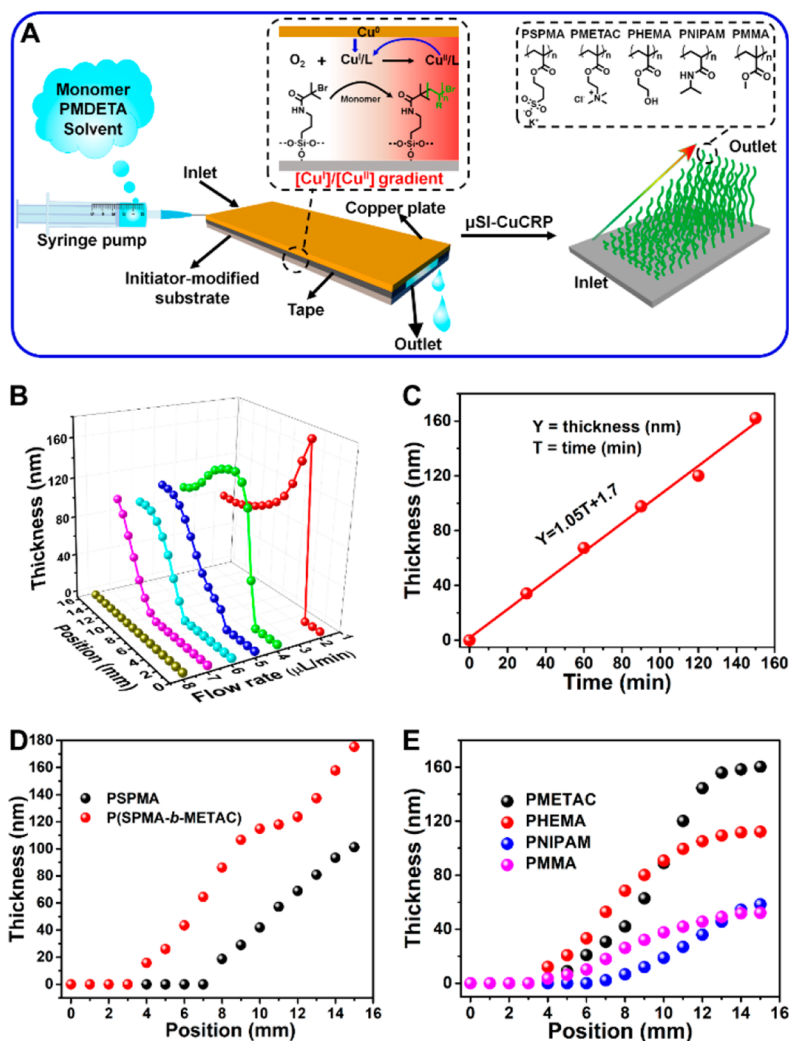


Figure 1. (A) Schematic view of the experimental setup of μ SI-CuCRP by using a syringe as the continuous reaction solution supplier. (B) PSPMA brush thickness profiles at various positions of different flow rates, polymerization time: 1 h. (C) Time-height dependence of the PSPMA brushes growth at the selected 13 mm position after the reinitiation. (D) Preparation of gradient P(SPMA-*b*-METAC) block copolymer brushes via sequential polymerization of SPMA and METAC. (E) Polymer brush thickness profiles at various positions with different monomers.

reducing agent for the Cu^{II} complex, regenerating the active Cu^{I} catalyst through the comproportionation. A Cu^{I} /ligand complex is generated in the vicinity of the initiator layer, reacts with initiator R-X generating radicals, and starts the polymerization when the reaction solution flows through the initiator layer.²⁴ The dissolved oxygen around the initiator is scavenged by Cu^{I} , while Cu^{I} is regenerated by the continuous reduction of Cu^{II} .^{25,26} It is also possible that the dissolved oxygen is scavenged via oxygen-consuming corrosion of metallic copper to form Cu_xO species and oxidation of Cu^{I} into Cu^{II} which act as a source of Cu^{I} and Cu^{II} . Meanwhile, a spatiotemporal concentration gradient of $[\text{Cu}^{\text{I}}]/[\text{Cu}^{\text{II}}]$ is formed as a function of the distance to the electrode and reaction time to mediate the polymerization kinetics of CuCRP (Figure 1A), as well as the gradient polymer brushes formation on the initiator-modified substrate.^{22,24} At the low flow rate, that is, a longer diffusion time produced a higher concentration of $[\text{Cu}^{\text{I}}]/[\text{Cu}^{\text{II}}]$ and a fast polymerization rate. However, termination reactions limit the maximum growth of the polymer brushes.^{27,28}

As a proof-of-concept, we investigated the polymerization of 3-sulfopropyl methacrylate potassium salt (SPMA) on the

ATRP initiator-modified Si wafer through the capillary μ SI-CuCRP.^{15,16} The influence of the flow rate on the morphology of polymer brushes was studied and the thickness of the gradient polymer brushes on the substrate was measured by ellipsometry. An area (or length) with the noncovered substrate can be observed depending on the respective flow rate (Figure S1). As shown in Figure 1B, the induction length (from the inlet to where polymer brushes grow) is 2 mm at the flow rate of 2 $\mu\text{L}/\text{min}$. As the flow rate increases, the induction length increases to 12 mm (8 $\mu\text{L}/\text{min}$). Due to the limited size (around 15 mm) of the wafer used, only a few nanometer-thick polymer brushes were grafted near the outlet for 8 $\mu\text{L}/\text{min}$. When the flow rate was above 8 $\mu\text{L}/\text{min}$, no polymer brush growth was observed. For a flow rate in between (5, 6, and 7 $\mu\text{L}/\text{min}$), gradient polymer brushes with different cover areas and steepness along with the flow direction were obtained. The closer the positions to the outlet, the higher the height of the polymer brushes. However, the profiles of the gradient polymer brushes prepared at the flow rate 5, 6, and 7 $\mu\text{L}/\text{min}$ are different from flow rate below 5 $\mu\text{L}/\text{min}$, a low flow rate leads to a high content of Cu^{I} species and, hence, heavy termination reactions can be expected. There is an induction

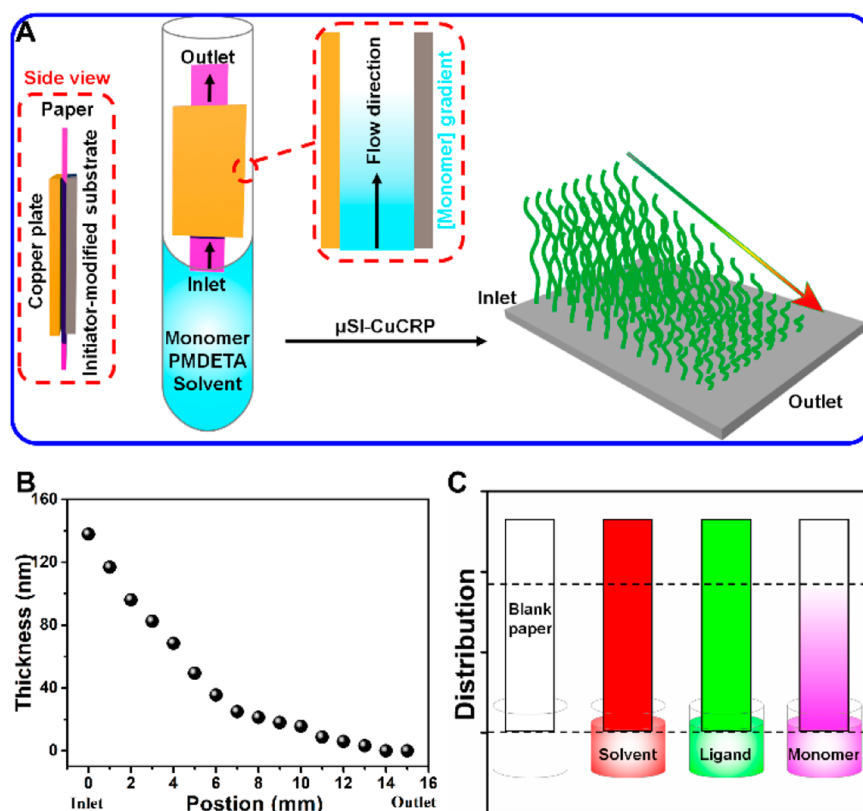


Figure 2. (A) Schematic view of the experimental setup of paper-based capillary μ SI-CuCRP. (B) PSPMA brush thickness profiles at various positions. (C) Illustration of the distribution of solvent, ligand, and monomer on paper during capillary μ SI-CuCRP.

period during which Cu^{I} is generated, and eventually the polymerization starts, a faster flow rate corresponds to lower Cu^{I} and limits polymer growth, which can be used for straightforward adjustment of grafting area as well as steepness of the gradient polymer brushes. We also examined the difference between capillary microfluidic and static (or stop-flow) SI-CuCRP of the SPMA monomer (Figure S2a). In static SI-CuCRP, no fresh oxygen was introduced, which yielded thicker and homogeneous polymer brushes. Thus, capillary μ SI-CuCRP can be used to guide the design of continuous reactors for solution-based CuCRP to study the induction period.²⁹

In order to demonstrate the high end-group fidelity of the polymers and the “living” nature of the capillary μ SI-CuCRP method, reinitiation of PSPMA was carried out, cycles of 30 min polymerization time were carried out. Thicknesses of the PSPMA at different positions after each cycle of the reinitiation exhibited a gradient growth along the flow route (Figure S3), resulting in controlled steepness of gradient by controlling the polymerization time. The time-height dependence of the PSPMA brushes at the 13 mm position was plotted in Figure 1C, the thickness of the polymer brushes at this position increased linearly with the polymerization cycles, the growth rate was about 1.05 nm/min. These results demonstrate the high end-group fidelity of the PSPMA brushes and the “living” nature of μ SI-CuCRP. Additionally, the copper plate can be reused many times and no decrease in polymer growth rate was observed. Further analysis at different positions was investigated to compare the growth rate of PSPMA brushes (Figure S4). Gradient block copolymer brushes of PSPMA and poly[2-(methacryloyloxy)ethyl] trimethylammonium chloride (PME-

TAC) were prepared. The thicknesses of PSPMA and P(SPMA-*b*-METAC) brushes are shown in Figure 1D, both the time-height dependence and the block copolymer brushes verified the “living” nature and air tolerance of the capillary μ SI-CuCRP.

In addition to the anionic SPMA monomer, other types of monomers such as thermoresponsive *N*-isopropylacrylamide (NIPAM), neutral hydrophilic HEMA and hydrophobic methyl methacrylate (MMA), and cationic METAC were successfully polymerized using the capillary μ SI-CuCRP. The brush thickness profiles of different gradient polymer brushes are presented in Figure 1E. METAC and HEMA showed similar polymerization behavior to SPMA. However, the thickness of PNIPAM and PMMA was relatively thinner than PSPMA, PMETAC, and PHEMA, due to the different polymerization nature of monomers.³⁰ Infrared spectroscopy (IR; Figure S6) and contact angle measurements (Figure S7) proved that polymers were successfully grafted onto the substrates. A wide range of monomers with different properties is applicable to the capillary μ SI-CuCRP. We also compared the thickness of the polymer brushes between capillary μ SI-CuCRP and the static SI-CuCRP (Figure S2), the different polymerization kinetics of the two methods can be ascribed to the amount of air in the polymerization solution. μ SI-CuCRP can also be used to prepare patterned gradient brushes by pre patterning the initiator on the substrate (Figure S8). The color changes indicate the different thickness of the polymer brushes.³¹

Since the pump-based capillary μ SI-CuCRP needs polydimethylsiloxane (PDMS) channels. In contrast, paper as an easily available material that can wick aqueous fluids without

external power has been widely exploited as microfluidic devices.^{32–36} We used paper instead of PDMS channels to prepare complex polymer brushes on the surface. Figure 2A illustrates the experimental process of the paper-based capillary μ SI-CuCRP, the filter paper was clamped between the initiator-modified substrate and the copper plate. Subsequently, one side of the paper was immersed in the reaction solution to replace the syringe pump by the capillary force of the paper, gradient polymer brushes were obtained after the polymerization. Counterintuitively, the gradient direction is different from that obtained by the syringe pump-based capillary μ SI-CuCRP. Figure 2B shows that the thickness of the gradient decreased from 138 nm to 0 along the flow direction. Control experiments were conducted, and the results are illustrated in Figure 2C. After 1 h of the polymerization time, both the solvent and PMDETA (stained with phenolphthalein) spread all over the paper. SPMA solution was oxidized with alkaline KMnO_4 solution and showed a gradient color change that is in accordance with the gradient in Figure 2B. The SPMA flow and the resulting gradient can be explained by the polarity mismatch of the eluent (SPMA) and quasi-stationary phase (cellulose).³⁷ The monomer concentration gradient along the flow direction led to the gradient polymer brush growth, steeper gradient was observed at longer polymerization time, while the polymer brush growth at the same position showed linear growth behavior which is similar to the traditional ATRP method (Figure S9). The pore size of the filter paper showed little effect on polymer brushes growth when it was above $0.8 \mu\text{m}$, but very limited polymer growth was observed ($\sim 40 \text{ nm}$), which is probably due to the low driving force for the monomer solution and high air content exists in the pores. Below this value, for example, $0.45 \mu\text{m}$, a faster polymerization rate and thicker polymer layer were observed (Figure S10).

To further elucidate the advantage of paper-based capillary μ SI-CuCRP, polymerization of multiple monomers on a single surface without using PDMS channels was carried out (Figure 3 top). A piece of paper was placed between the substrate and the copper plate, the two sides of the paper were immersed in

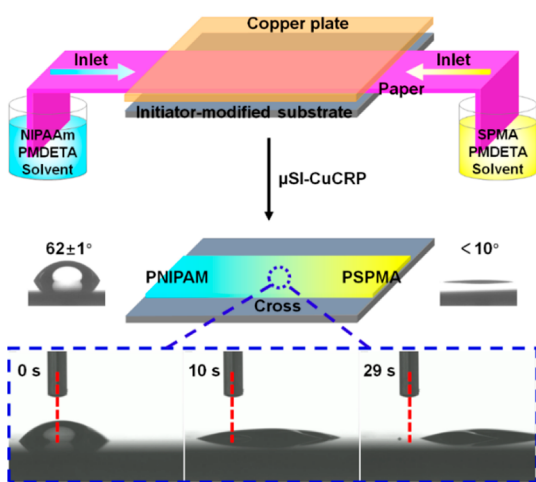


Figure 3. Illustration of simultaneous preparation of two polymer brushes via paper-based capillary μ SI-CuCRP (top), the mixed polymer brush gradients and wettability at different positions (middle), as well as the mobility of water in the middle of the substrate, where two mixed polymer brushes grafted (bottom), pore size of the filter paper: $0.45 \mu\text{m}$.

different polymerization solutions (e.g., SPMA and NIPAM), binary polymer brushes were grafted on the same substrate after 1h. Contact angle measurements were used to characterize the wettability of the mixed polymer brushes. In the PNIPAM region, the contact angle (CA) was $62 \pm 1^\circ$, and the CA was below 10° in the PSPMA region (Figure 3, middle). Interestingly, in the middle where PNIPAM and PSPMA meet, directed water flow from PNIPAM to PSPMA (Figure 3, bottom) was observed, the driving force for the droplet can be attributed to the different hydrophilicity of two polymer brushes. Capillary μ SI-CuCRP provides a simple way to study the interfacial properties of different polymer brushes and to prepare substrates with directed motility of droplets.³⁸

Furthermore, patterned polymer brushes were also prepared via paper-based capillary μ SI-CuCRP. In combination with other patterning technologies (e.g., photolithography),³⁹ patterned polymer brushes with different shapes and micro-scale size were fabricated (Figure 4A–C). AFM image of the

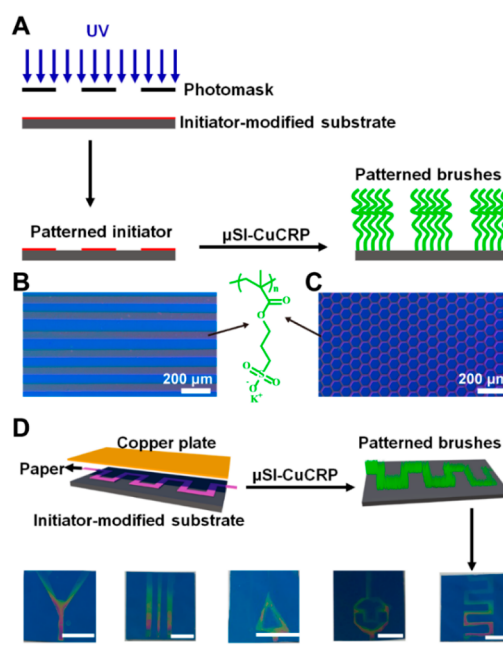


Figure 4. (A) Illustration of negative patterning of PSPMA brushes via paper-based capillary μ SI-CuCRP, the pore size of the filter paper: $0.45 \mu\text{m}$. (B, C) Optical micrographs of patterned PSPMA brushes. (D) Preparation of patterned polymer brushes by using different shaped paper cutting and the resultant patterns of the PSPMA brushes on a Si wafer (scale bar: 5 mm).

patterned polymer brushes shows the pattern formation with well-defined structures (Figure S11). As the solution flows along the paper driven by the capillary force, the shape of the paper determines the shape of the polymer brush pattern without pre patterning the surface with the ATRP initiator. Various shapes (curve, polymer brush array, triangle, Y shape, or complex logo) of polymer brushes on homogeneous initiator layers were created by simply cutting the paper into desired shapes (Figures 4D and S12). Thus, paper-based capillary μ SI-CuCRP provides a very easy way to fabricate the polymer brush arrays. Within the polymer brush array, the color change indicates the thickness of the polymer brushes.

In conclusion, a facile and universal capillary microfluidic-assisted polymer brush synthesis and surface structuring

technology, capillary μ SI-CuCRP was developed. Gradient polymer brushes with controllable steepness, thickness, and grafting area can be easily obtained via μ SI-CuCRP by adjusting the flow rate and the polymerization time. In addition, time-height dependence and block copolymer brush gradients demonstrated the high chain-end group fidelity of the polymers and the “living” nature of capillary μ SI-CuCRP. Complex polymer brush patterns were successfully fabricated by combining paper cutting and lithography technologies. Binary polymer brushes were also grown simultaneously from both ends of the same paper strip, which might be used to study the interfacial properties of different polymer brushes and study the droplet motility on the gradient surface. This surface polymerization method opens a new way for surface structuring.

■ ASSOCIATED CONTENT

Supporting Information

The Supporting Information is available free of charge at <https://pubs.acs.org/doi/10.1021/acsmacrolett.9b00921>.

Experimental details and additional characterization data (PDF)

■ AUTHOR INFORMATION

Corresponding Authors

Bin Li – Physik Department, TUM – Technische Universität München, 85748 Garching, Germany; orcid.org/0000-0001-6696-5049; Email: bin1.li@tum.de

Tao Zhang – Key Laboratory of Bio-based Polymeric Materials Technology and Application of Zhejiang Province, Ningbo Institute of Material Technology and Engineering Chinese Academy of Sciences, Ningbo 315201, China; University of Chinese Academy of Sciences, Beijing 100049, China; orcid.org/0000-0003-3218-0571; Email: tao.zhang@tu-dresden.de

Rainer Jordan – Chair of Macromolecular Chemistry, Faculty of Chemistry and Food Chemistry, School of Science, Technische Universität Dresden, 01069 Dresden, Germany; orcid.org/0000-0002-9414-1597; Email: rainer.jordan@tu-dresden.de

Authors

Wei Li – Chair of Macromolecular Chemistry, Faculty of Chemistry and Food Chemistry, School of Science, Technische Universität Dresden, 01069 Dresden, Germany

Wenbo Sheng – Chair of Macromolecular Chemistry, Faculty of Chemistry and Food Chemistry, School of Science, Technische Universität Dresden, 01069 Dresden, Germany

Erik Wegener – Chair of Macromolecular Chemistry, Faculty of Chemistry and Food Chemistry, School of Science, Technische Universität Dresden, 01069 Dresden, Germany

Yunhao Du – Chair of Macromolecular Chemistry, Faculty of Chemistry and Food Chemistry, School of Science, Technische Universität Dresden, 01069 Dresden, Germany

Complete contact information is available at: <https://pubs.acs.org/doi/10.1021/acsmacrolett.9b00921>

Notes

The authors declare no competing financial interest.

■ ACKNOWLEDGMENTS

W.L. acknowledges financial support from the China Scholarship Council (CSC) of the People's Republic of China (Ph.D.

Grant). W.S. acknowledges Ph.D. research funding from the Initiative and Networking Fund of the Helmholtz Association of German Research Centers through the International Helmholtz Research School for Nanoelectronic Networks, IHRS NANONET (VH-KO-606). T.Z. acknowledges the Ningbo “3315 Innovation Programme” (No. 2019-17-C).

■ REFERENCES

- (1) Zoppe, J. O.; Ataman, N. C.; Mocny, P.; Wang, J.; Moraes, J.; Klok, H.-A. Surface-Initiated Controlled Radical Polymerization: State-of-the-Art, Opportunities, and Challenges in Surface and Interface Engineering with Polymer Brushes. *Chem. Rev.* **2017**, *117*, 1105–1318.
- (2) Ma, S.; Zhang, X.; Yu, B.; Zhou, F. Brushing up Functional Materials. *NPG Asia Mater.* **2019**, *11*, 24.
- (3) Yang, W.; Zhou, F. Polymer Brushes for Antibiofouling and Lubrication. *Biosurf. Biotribol.* **2017**, *3*, 97–114.
- (4) Wang, J.-S.; Matyjaszewski, K. Controlled/“Living” Radical Polymerization. Halogen Atom Transfer Radical Polymerization Promoted by a Cu (I)/Cu (II) Redox Process. *Macromolecules* **1995**, *28*, 7901–7910.
- (5) Tomlinson, M. R.; Genzer, J. Formation of Grafted Macromolecular Assemblies with a Gradual Variation of Molecular Weight on Solid Substrates. *Macromolecules* **2003**, *36*, 3449–3451.
- (6) Xu, C.; Wu, T.; Drain, C. M.; Batteas, J. D.; Beers, K. L. Microchannel Confined Surface-Initiated Polymerization. *Macromolecules* **2005**, *38*, 6–8.
- (7) Xu, C.; Barnes, S. E.; Wu, T.; Fischer, D. A.; DeLongchamp, D. M.; Batteas, J. D.; Beers, K. L. Solution and Surface Composition Gradients Via Microfluidic Confinement: Fabrication of a Statistical-Copolymer-Brush Composition Gradient. *Adv. Mater.* **2006**, *18*, 1427–1430.
- (8) Sheng, W.; Li, B.; Wang, X.; Dai, B.; Yu, B.; Jia, X.; Zhou, F. Brushing up from “Anywhere” under Sunlight: A Universal Surface-Initiated Polymerization from Polydopamine-Coated Surfaces. *Chem. Sci.* **2015**, *6*, 2068–2073.
- (9) Matyjaszewski, K. Advanced Materials by Atom Transfer Radical Polymerization. *Adv. Mater.* **2018**, *30*, 1706441.
- (10) Navarro, L. A.; Enciso, A. E.; Matyjaszewski, K.; Zauscher, S. Enzymatically Degassed Surface-Initiated Atom Transfer Radical Polymerization with Real-Time Monitoring. *J. Am. Chem. Soc.* **2019**, *141*, 3100–3109.
- (11) Li, M.; Fromel, M.; Ranaweera, D.; Rocha, S.; Boyer, C.; Pester, C. W. Si-Pet-Raft: Surface-Initiated Photoinduced Electron Transfer-Reversible Addition–Fragmentation Chain Transfer Polymerization. *ACS Macro Lett.* **2019**, *8*, 374–380.
- (12) Wang, C. G.; Chen, C.; Sakakibara, K.; Tsujii, Y.; Goto, A. Facile Fabrication of Concentrated Polymer Brushes with Complex Patterning by Photocontrolled Organocatalyzed Living Radical Polymerization. *Angew. Chem., Int. Ed.* **2018**, *57*, 13504–13508.
- (13) Narupai, B.; Page, Z. A.; Treat, N. J.; McGrath, A. J.; Pester, C. W.; Discekici, E. H.; Dolinski, N. D.; Meyers, G. F.; Read de Alaniz, J.; Hawker, C. J. Simultaneous Preparation of Multiple Polymer Brushes under Ambient Conditions Using Microliter Volumes. *Angew. Chem., Int. Ed.* **2018**, *57*, 13433–13438.
- (14) Yan, J.; Li, B.; Zhou, F.; Liu, W. Ultraviolet Light-Induced Surface-Initiated Atom-Transfer Radical Polymerization. *ACS Macro Lett.* **2013**, *2*, 592–596.
- (15) Zhang, T.; Du, Y.; Müller, F.; Amin, I.; Jordan, R. Surface-Initiated Cu(0) Mediated Controlled Radical Polymerization (SI-CuCRP) Using a Copper Plate. *Polym. Chem.* **2015**, *6*, 2726–2733.
- (16) Zhang, T.; Du, Y.; Kalbacova, J.; Schubel, R.; Rodriguez, R. D.; Chen, T.; Zahn, D. R. T.; Jordan, R. Wafer-Scale Synthesis of Defined Polymer Brushes under Ambient Conditions. *Polym. Chem.* **2015**, *6*, 8176–8183.
- (17) Liarou, E.; Whitfield, R.; Anastasaki, A.; Engelis, N. G.; Jones, G. R.; Velonia, K.; Haddleton, D. Copper Mediated Polymerization

without External Deoxygenation or Oxygen Scavengers. *Angew. Chem., Int. Ed.* **2018**, *57*, 8998–9002.

(18) Che, Y.; Zhang, T.; Du, Y.; Amin, I.; Marschelke, C.; Jordan, R. "On Water" Surface-Initiated Polymerization of Hydrophobic Monomers. *Angew. Chem., Int. Ed.* **2018**, *57*, 16380–16384.

(19) Zhang, T.; Benetti, E. M.; Jordan, R. Surface-Initiated Cu(0)-Mediated CRP for the Rapid and Controlled Synthesis of Quasi-3d Structured Polymer Brushes. *ACS Macro Lett.* **2019**, *8*, 145–153.

(20) Yan, J.; Li, B.; Yu, B.; Huck, W. T.; Liu, W.; Zhou, F. Controlled Polymer-Brush Growth from Microliter Volumes Using Sacrificial-Anode Atom-Transfer Radical Polymerization. *Angew. Chem., Int. Ed.* **2013**, *52*, 9125–9129.

(21) Shida, N.; Koizumi, Y.; Nishiyama, H.; Tomita, I.; Inagi, S. Electrochemically Mediated Atom Transfer Radical Polymerization from a Substrate Surface Manipulated by Bipolar Electrolysis: Fabrication of Gradient and Patterned Polymer Brushes. *Angew. Chem.* **2015**, *127*, 3994–3998.

(22) Li, B.; Yu, B.; Huck, W. T.; Liu, W.; Zhou, F. Electrochemically Mediated Atom Transfer Radical Polymerization on Nonconducting Substrates: Controlled Brush Growth through Catalyst Diffusion. *J. Am. Chem. Soc.* **2013**, *135*, 1708–1710.

(23) Li, B.; Yu, B.; Huck, W. T.; Zhou, F.; Liu, W. Electrochemically Induced Surface-Initiated Atom-Transfer Radical Polymerization. *Angew. Chem., Int. Ed.* **2012**, *51*, 5092–5095.

(24) Dehghani, E. S.; Du, Y.; Zhang, T.; Ramakrishna, S. N.; Spencer, N. D.; Jordan, R.; Benetti, E. M. Fabrication and Interfacial Properties of Polymer Brush Gradients by Surface-Initiated Cu(0)-Mediated Controlled Radical Polymerization. *Macromolecules* **2017**, *50*, 2436–2446.

(25) Li, B.; Yu, B.; Ye, Q.; Zhou, F. Tapping the Potential of Polymer Brushes through Synthesis. *Acc. Chem. Res.* **2015**, *48*, 229–237.

(26) Fantin, M.; Ramakrishna, S. N.; Yan, J.; Yan, W.; Divandari, M.; Spencer, N. D.; Matyjaszewski, K.; Benetti, E. M. The Role of Cu⁰ in Surface-Initiated Atom Transfer Radical Polymerization: Tuning Catalyst Dissolution for Tailoring Polymer Interfaces. *Macromolecules* **2018**, *51*, 6825–6835.

(27) Li, B.; Yu, B.; Zhou, F. In Situ AFM Investigation of Electrochemically Induced Surface-Initiated Atom-Transfer Radical Polymerization. *Macromol. Rapid Commun.* **2013**, *34*, 246–250.

(28) Fantin, M.; Isse, A. A.; Gennaro, A.; Matyjaszewski, K. Understanding the Fundamentals of Aqueous ATRP and Defining Conditions for Better Control. *Macromolecules* **2015**, *48*, 6862–6875.

(29) Hu, X.; Zhu, N.; Fang, Z.; Li, Z.; Guo, K. Continuous Flow Copper-Mediated Reversible Deactivation Radical Polymerizations. *Eur. Polym. J.* **2016**, *80*, 177–185.

(30) Jones, D. M.; Huck, W. T. S. Controlled Surface-Initiated Polymerizations in Aqueous Media. *Adv. Mater.* **2001**, *13*, 1256–1259.

(31) Qin, M.; Sun, M.; Bai, R.; Mao, Y.; Qian, X.; Sikka, D.; Zhao, Y.; Qi, H. J.; Suo, Z.; He, X. Bioinspired Hydrogel Interferometer for Adaptive Coloration and Chemical Sensing. *Adv. Mater.* **2018**, *30*, 1800468.

(32) Gong, M. M.; Sinton, D. Turning the Page: Advancing Paper-Based Microfluidics for Broad Diagnostic Application. *Chem. Rev.* **2017**, *117*, 8447–8480.

(33) Ainla, A.; Hamed, M. M.; Güder, F.; Whitesides, G. M. Electrical Textile Valves for Paper Microfluidics. *Adv. Mater.* **2017**, *29*, 1702894–1702903.

(34) Guo, Z. H.; Jiao, Y. C.; Wang, H. L.; Zhang, C.; Liang, F.; Liu, J. L.; Yu, H. D.; Li, C. M.; Zhu, G.; Wang, Z. L. Self-Powered Electrowetting Valve for Instantaneous and Simultaneous Actuation of Paper-Based Microfluidic Assays. *Adv. Funct. Mater.* **2019**, *29*, 1808974.

(35) Hamed, M. M.; Ainla, A.; Güder, F.; Christodouleas, D. C.; Fernandez-Abedul, M. T.; Whitesides, G. M. Integrating Electronics and Microfluidics on Paper. *Adv. Mater.* **2016**, *28*, 5054–5063.

(36) Yamada, K.; Henares, T. G.; Suzuki, K.; Citterio, D. Paper-Based Inkjet-Printed Microfluidic Analytical Devices. *Angew. Chem., Int. Ed.* **2015**, *54*, 5294–5310.

(37) Wendenburg, S.; Nachbar, M.-L.; Biesalski, M. Tailoring the Retention of Charged Model Compounds in Polymer Functionalized Paper-Based Microfluidic Devices. *Macromol. Chem. Phys.* **2017**, *218*, 1600408–1600422.

(38) Chaudhury, M. K.; Whitesides, G. M. How to Make Water Run Uphill. *Science* **1992**, *256*, 1539–1541.

(39) Chen, T.; Amin, I.; Jordan, R. Patterned Polymer Brushes. *Chem. Soc. Rev.* **2012**, *41*, 3280–3296.